Electrical Solitons for Microwave Systems

David S. Ricketts, En Shi, Xiaofeng Li, Nan Sun, O. Ozgur Yildirim, and Donhee Ham

Nonlinearity and dispersion are often nuisances that microwave engineers seek to curb. However, there is a system that can harmonize these two effects to produce useful—and fascinating—dynamics with unique microwave engineering opportunities: the nonlinear transmission line (NLTL) [1]–[11]. The NLTL is a ladder network of lumped inductors and varactors [Figure 1(a)] that can be alternatively built by periodically loading a smooth transmission line with lumped varactors [Figure 1(b)].

The NLTL is a nonlinear dispersive medium. On one hand, it exhibits nonlinearity due to the varactors, which are typically realized as reverse-biased p-n junctions or Schottky diodes; their voltage-dependent capacitance is responsible for the nonlinearity. On the other hand, the NLTL is dispersive due to its structural periodicity. This periodicity makes the NLTL a low-pass filter with a cutoff frequency near which the NLTL becomes increasingly dispersive. The star of the harmony between nonlinearity and dispersion is the soliton [12]–[14], a bell-shaped traveling voltage pulse [Figure 1(c)], where nonlinearity and dispersion exactly counteract each other. Due to this balancing act, the soliton neither spreads (no dispersion) nor steepens to form a shock wavefront (no nonlinearity). It propagates down the line, preserving its shape, at least in the absence of loss.

A Brief History of the Physics of Solitons

The soliton is a phenomenon observed broadly in nature beyond the electrical domain, with hydrodynamic solitons on the surface of shallow water being a prominent example [13], [14]. From our experience, it is easy to see that water can be a nonlinear dispersive medium. On one hand, a stone thrown in water may initially create a pulse, which would then spread because different frequency components of the initial pulse travel at different speeds (dispersion). On the other hand, an ocean wave gently rolling in from a distance can crest and crash on the shore; this breaking on the shore occurs because the speed difference between

David S. Ricketts (david.ricketts@ncsu.edu) is with the Department of Electrical and Computer Engineering, North Carolina State University, Raleigh, United States. En Shi is with the Department of Electrical and Computer Engineering, Carnegie Mellon University, Pittsburgh, Pennsylvania, United States. Xiaofeng Li (llxxff@gmail.com) is with Element Capital Management, New York, United States. Nan Sun (nansun@mail.utexas.edu) is with the Department of Electrical and Computer Engineering, University of Austin, Texas, United States. O. Ozgur Yildirim (oozgury@gmail.com) is with Lightmatter, Boston, Massachusetts, United States. Donhee Ham (donhee@seas.harvard.edu) is with Applied Physics and Electrical Engineering, Harvard University, Cambridge, Massachusetts, United States.

Digital Object Identifier 10.1109/MMM.2019.2891382
Date of publication: 7 March 2019

the faster top and slower bottom portions of the wave becomes increasingly pronounced as the water depth is reduced on the shore (nonlinearity). Therefore, the shallow water is a medium in which nonlinearity and dispersion manifest together and can support hydrodynamic soliton propagation, just as the NLTL is a nonlinear dispersive medium that supports electrical (voltage) soliton propagation.

The soliton was, in fact, first discovered in hydrodynamic form in 1834, as John Scott Russell watched a barge being towed in the Edinburgh–Glasgow Canal [15]. The tow cable snapped, and the prow dropped, which created a heap of water to propagate down the canal. Russell, on horseback, followed this "solitary" wave for several kilometers, noticing that the water pulse did not spread. This lack of dispersion was due to the counteracting effect of nonlinearity, but the underlying mechanism would not be understood until much later. For example, it was more than 40 years later (in 1877) that Boussinesq introduced a partial differential equation to describe the wave dynamics in the nonlinear dispersive medium, and in 1895 Korteweg and de Vries rediscovered this partial differential equation, which is now celebrated as the Korteweg–de Vries (KdV) equation bearing their names [16]. It is typically written in the following simplified form:

$$\partial u/\partial t + 6u\partial u/\partial x + \partial^3 u/\partial x^3 = 0, \tag{1}$$

where u is the wave amplitude and t and x are the time and position variables of the wave. Physical parameters, such as density, gravity, and tension relevant for the water wave dynamics, are not show in (1), because

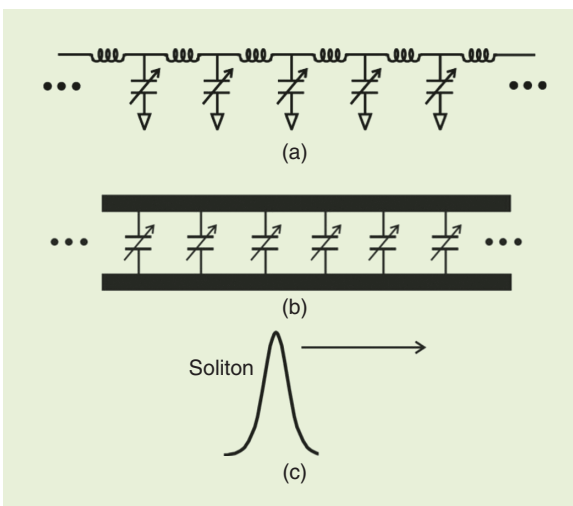

Figure 1. *(a) The NLTL consists of lumped inductors and varactors. (b) The NLTL can be alternatively built by periodically loading a smooth transmission line with lumped varactors. (c) A soliton pulse propagates down the NLTL, preserving its shape.*

u, t, and x here are made all dimensionless after absorbing the physical parameters through rescaling. The KdV equation was then found to admit, as its particular solution, the following bell-shaped traveling monopulse [13], [14]:

$$u(x,t) = A\,\mathrm{sech}^2\left[(A/2)^{\frac{1}{2}}(x-2At)\right], \tag{2}$$

where A is an arbitrary parameter. For a given value of A, this traveling pulse has a fixed shape with the time-independent amplitude (A), width ($\propto (2/A)^{1/2}$), and velocity ($2A$) [1], and it neither sharpens nor spreads with time. A is the parameter that defines a given pulse, determining its amplitude, width, and velocity. One can also see that a taller pulse is narrower and travels faster. This monopulse solution modeled well the solitary wave Russell observed.

This solitary wave did not come to be called the *soliton* until the seminal work by Zabusky and Kruskal in 1965 [17]. In their numerical simulation of an initial-condition problem for the KdV equation, they observed that an initially nonsolitary wave profile (e.g., sinusoid) on a nonlinear dispersive medium evolves into multiple solitary pulses. Furthermore, these solitary pulses act like particles, in the sense that they remarkably maintain their identities even after they pass through one another with strong nonlinear interactions. It was this particle-like behavior that led Zabusky and Kruskal to coin the name *soliton* for the solitary pulse. In 1967 and 1968, Gardner, Greene, Kruskal, and Miura at Princeton University applied an analytical framework known as the *inverse scattering method* to the initial-condition KdV problem of how an arbitrary wave launched onto a nonlinear dispersive medium evolves into multiple solitons [18], [19]. Their study unveiled the fundamental mathematical structure underlying the KdV dynamics. The inverse scattering method, subsequently generalized by Lax in 1968 [20], was a landmark development in 20th-century mathematical physics.

Wave Dynamics on the Nonlinear Dispersive Medium

A transmission line consisting of two (or more) metals smoothly running in parallel is a good approximation of a linear, nondispersive medium. It is linear unless the signal is so excessively large as to provoke the weak nonlinearity of the dielectric material between the two metals. It is nondispersive, at least from the structural point of view, in that it has no lumped periodicity like the NLTL. An input wave of an arbitrary shape launched onto this linear, nondispersive line maintains its shape in the course of propagation. The input wave can be decomposed into sinusoidal components. Each

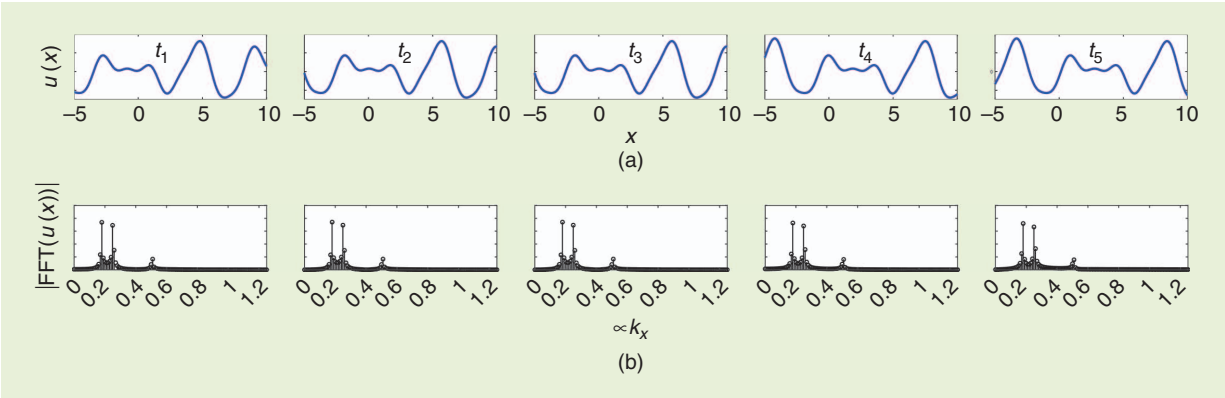

Figure 2. *(a) Simulated signal propagation on a linear, nondispersive medium. The spatial waveform u(x) at five different time instants is shown. (b) The Fourier transform of u(x) at the five different time instants. Here, the horizontal axis is proportional to the wave number k_x. All component sinusoids are preserved. FFT: fast Fourier transform.*

sinusoid, labeled by a frequency, keeps its amplitude constant as the wave travels—that is, each component sinusoid is preserved, so the spectrum of the wave remains the same. Figure 2 shows a simulated example of the time evolution of a linear, nondispersive wave consisting of three component sinusoids.

We now consider a simulated wave propagation on an NLTL [Figure 3(a)], where a nonsoliton wave [red waveform, which does not conform to (2)] is launched onto the NLTL. Because the nonlinearity and dispersion of the NLTL are not balanced for this initial nonsoliton wave, it will change shape while traveling. The blue waveform in Figure 3(a) is a snapshot of the wave after propagating down the NLTL for a short time: the shape change from the initial red waveform is evident. In the frequency domain, the spectral makeup of the wave correspondingly changes, with amplitudes of existing frequency components being altered and new frequency components being created. Specifically, the blue waveform contains a faster rise and a faster fall than the red waveform, corresponding to the generation of higher-frequency components, which is explicitly seen in the frequency domain [Figure 3(b)]. In summary, the component sinusoids of a nonsoliton input to the NLTL are not preserved with time. This change in the frequency components is one key application of the NLTL in microwave systems, because a low-frequency nonsoliton input signal launched onto the NLTL can create higher-frequency spectral contents.

However, the nonsoliton wave that changes its waveform traveling down the NLTL still has preserved components. The three pulses contained in the blue waveform of Figure 3(a) are three solitons, each following the form of (2) with its respective value for the parameter A. That is, the shape change during the wave propagation is the process by which the nonsoliton input breaks into its component solitons. All individual component solitons nested in the initial nonsoliton

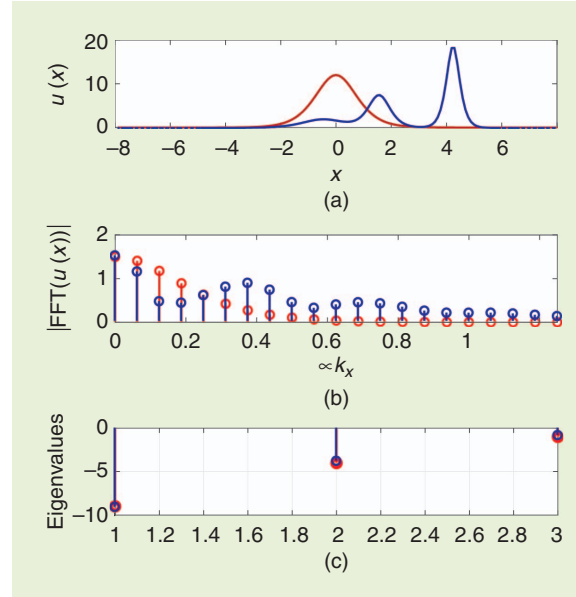

Figure 3. *Simulated dynamics on a nonlinear, dispersive medium using (1). (a) The spatial waveform u(x) is shown at two time instances. From an initial nonsoliton input (red waveform), three component solitons (blue waveform) break out. (b) The Fourier transform of u(x) at the two time instances with the horizontal axis being proportional to the wave number k_x. The spectral contents change with time. (c) The three eigenvalues tagging the three component solitons remain constant with time.*

waveform eventually emerge over time, with a taller soliton traveling faster than a shorter soliton. It is these component solitons that are preserved throughout time despite the overall waveform change [13], [14], [18]–[20].

Each component soliton of the nonlinear dispersive wave is labeled by a time-independent characteristic number, or a time-independent eigenvalue [Figure 3(c)], just as each component sinusoid of a linear wave is identified by a frequency. The eigenvalue labeling a particular

Russell, on horseback, followed this "solitary" wave for several kilometers, noticing that the water pulse did not spread.

soliton is another representation of the parameter A in (2) that defines that particular soliton. Owing to the constant eigenvalue or the constancy of the related value of A, each component soliton of the nonlinear dispersive wave maintains its shape, just as each component sinusoid of the linear wave maintains its amplitude. An arbitrary nonsoliton input wave launched onto the NLTL separates out into a sequence of component solitons of monotonically decreasing amplitudes and velocities, and, at any time during this overall waveform–changing process, each individual component soliton preserves its shape and identity, labeled by its time-independent eigenvalue [Figure 3(c)].

How do we obtain these time-independent eigenvalues by which to identify individual component solitons? To explain this fully, we must tell story of the inverse scattering method, for which we refer the interested reader to well-known texts, such as [13] and [14], or to original works, such as [18]–[20]. The crux of the story is that the set of time-independent eigenvalues is determined by the input wave launched onto the nonlinear dispersive medium, and the inverse scattering method will calculate all of the time-independent eigenvalues for the given input waveform, thus predicting how many and what shapes of (determined by the parameter A) solitons will emerge. Because the eigenvalues are time independent, their corresponding soliton components maintain their identities.

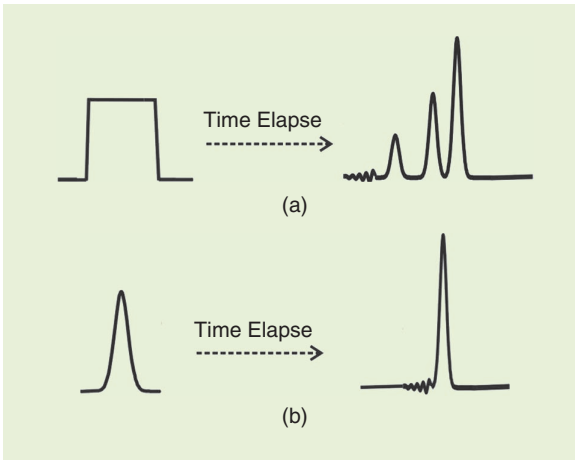

Figure 4. *A hypothetical illustration of (a) a square pulse breaking into three solitons and (b) a pulse close to a soliton solution evolving into that single soliton, both on a nonlinear dispersive medium.*

Figure 3(a) shows the bell-shaped nonsoliton input breaking into three component solitons. Figure 4(a) illustrates a square-shaped nonsoliton input breaking into three component solitons, with the extra energy that cannot be captured by the three solitons being shed as a dispersive tail (ringing). If a nonsoliton input wave is close enough to a soliton solution of the medium, it will evolve into that single soliton, while shedding extra energy as a dispersive tail [Figure 4(b)].

Soliton Collisions

Let a tall soliton initially propagate behind a short soliton along the same direction. As the tall soliton moves faster than the short soliton, the former will catch up with the latter (Figures 5 and 6). What happens when the two solitons meet? First, they distort in shape: this is not a linear superposition, but a nonlinear distortion with a strong interaction between the two solitons (Figures 5 and 6). In general, the merged amplitude is different from the linear sum of the amplitudes of the two solitons. Surprisingly, however, after this strong interaction, the two solitons reemerge with their original shapes intact and part ways, with the tall soliton now racing ahead of the short soliton (Figures 5 and 6). Therefore, the solitons act like particles: they smack into each other to distort their shapes, but then they recover their original shapes and continue on their way. In this sense, the encounter between the two solitons may be thought of as a collision.

During these collision dynamics, the overall waveform subsuming both solitons continues to be altered, because the intersoliton distance keeps changing and the two solitons distort during collision. The KdV equation governs this overall waveform change; at the same time, the KdV equation, via the inverse scattering method, yields two time-independent eigenvalues that label the tall and short solitons at any time instant (Figure 5). This identifiability of the individual solitons by the eigenvalues is consistent with the particle point of view.

Although the two solitons survive the collision, reemerging intact and in shape afterwards, the collision leaves a permanent mark through a time shift. That is, after the collision, each soliton acquires a permanent time shift. In the example shown in Figure 6, the tall and short solitons experience retardation and expedition in speed during the collision so that, after the collision, the tall and short solitons appear delayed and advanced, respectively, compared with the case of no collision.

Applications of the NLTL and Electrical Solitons

The NLTL was first introduced by Rolf Landauer at IBM in the 1960s for parametric amplification [2], but it was

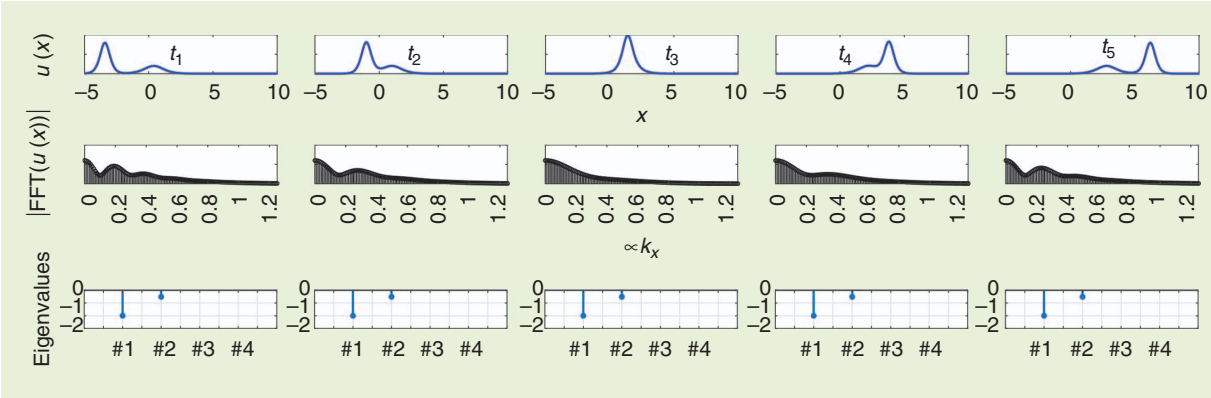

Figure 5. *When two solitons collide on a nonlinear, dispersive medium, the spectral content of the overall wave subsuming both solitons continues to change, but the two soliton eigenvalues are conserved. This is consistent with the particle point of view for the solitons.*

later realized that the nonlinear dispersive dynamics in the NLTL can be modeled using the KdV equation. The NLTL has since served not only as an easily accessible test bed for experimenting with a variety of KdV dynamics but also as a practical device in the forefront of ultrafast electronics applications, especially in high-speed measurement and high-frequency generation.

For example, the NLTL has enabled 100-GHz sampling in oscilloscopes [21]; NLTLs have been used to enable a bandwidth of 110 GHz in a vector network analyzer [22]; and harmonic generation is also enabled by NLTLs, with companies offering comb frequency generators [23], [24]. We will provide an overview of a few select cutting-edge applications of the electrical solitons and the NLTL.

Edge Sharpening

Consider an NLTL with a total physical length of l, consisting of N lumped inductor-varactor sections with each individual inductance being L and each varactor capacitance being $C(V)$; here, V signifies the reverse-bias voltage applied to the varactor, which is the line voltage where the varactor connects. For the reverse-biased p-n junction or Schottky diode, which is a typical choice for the varactor, $C(V)$ is lowered with an increasing V. From the theory of the linear discrete transmission line, we can readily state that the velocity of a small-signal wave modulated around a voltage V is given by $(l/N) \times [LC(V)]^{-1/2}$, well below the cutoff frequency.

Calculating the velocity of the large-signal soliton in terms of the circuit parameters is a much more involved process, entailing the solution of the full KdV equation, but the small-signal model can provide a valuable, albeit approximate, insight into the large-signal dynamics. In particular, the nonlinear velocity formula predicts that, if a slowly falling edge is launched onto the NLTL, the

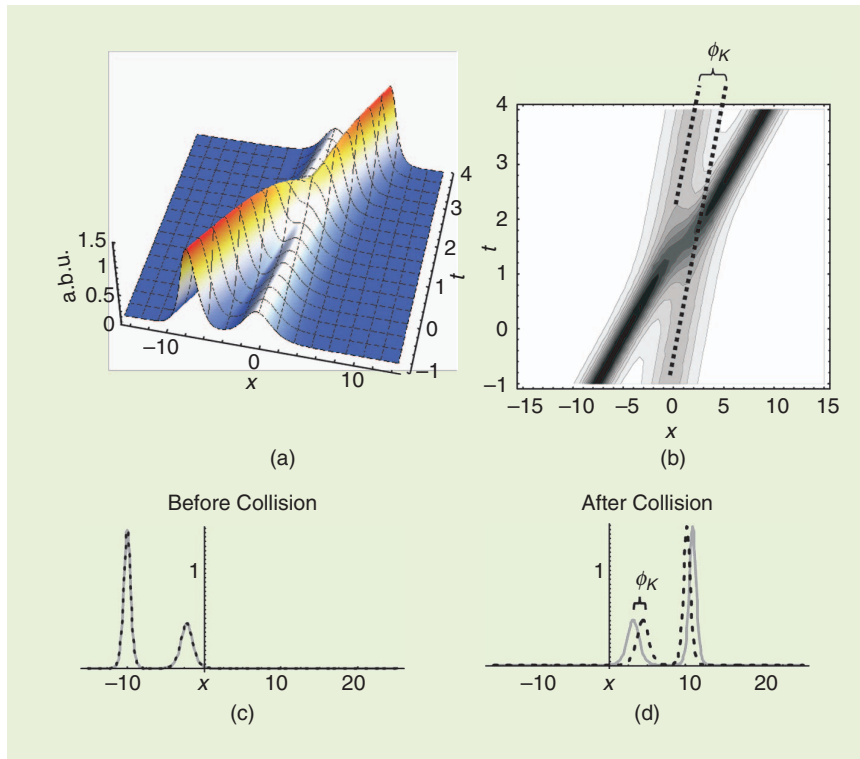

Figure 6. *(a)–(d) When two solitons collide on a nonlinear, dispersive medium, their shapes distort, but they reemerge from the collision with their shapes intact. However, the collision leaves a permanent time shift for each soliton. a.b.u.: arbitrary unit.*

top of the edge with a larger V, and thus a smaller $C(V)$, will travel faster than the bottom [Figure 7(a)]––just like a breaking wave on the shore in the ocean––thus sharpening the edge. This reduces the fall time of the edge, adding higher-frequency components to the signal.

This edge sharpening stops when the spectral contents of the falling edge are increased toward the cutoff frequency of the NLTL. Here, there are two cutoff frequencies to consider. We have already mentioned the one that arises from the low-pass filter nature of the NLTL with its structural periodicity: formally, this intrinsic cutoff frequency is called the *Bragg frequency* and is given by $w_{\text{Bragg}} = 2[LC(V)]^{-½}$. The expression here has the voltage dependency due to the nonlinearity, from which we can estimate the range of cutoff frequencies for a given $C(V)$ profile. The expression also indicates that a smaller inductor and/or a smaller varactor would increase w_{Bragg}. The other cutoff frequency arises from the dissipation in the NLTL. If we assume that the skin effect of each line inductor is the main source of loss, the inductor L of each section of the NLTL would be accompanied by a series resistance R, and the corresponding loss-based cutoff frequency would be the RC filter bandwidth, $w_{RC} \sim 1/(RC)$.

If w_{RC} is much larger than w_{Bragg} (weak loss regime), the nonlinear edge sharpening will be checked by the NLTL's dispersion effect, but this can create solitons and ringing [Figure 7(b), left]. In contrast, if w_{RC} becomes comparable to w_{Bragg} (strong loss regime), loss becomes important in checking the nonlinear edge sharpening [Figure 7(b), right]. In this case, the edge simply stops getting sharper without generating solitons and ringing. By increasing both w_{RC} and w_{Bragg} together in the strong loss regime, one then would be able to form sharper and sharper edges. In 1994, van der Weide realized an integrated NLTL in gallium arsenide (GaAs) technology, with reverse-biased Schottky diodes serving as varactors, and exploited the NLTL's edge-sharpening ability to achieve a record 430-fs falling edge [6]. NLTL edge sharpening has been leveraged in commercial products, such as a 110-GHz vector network analyzer [22].

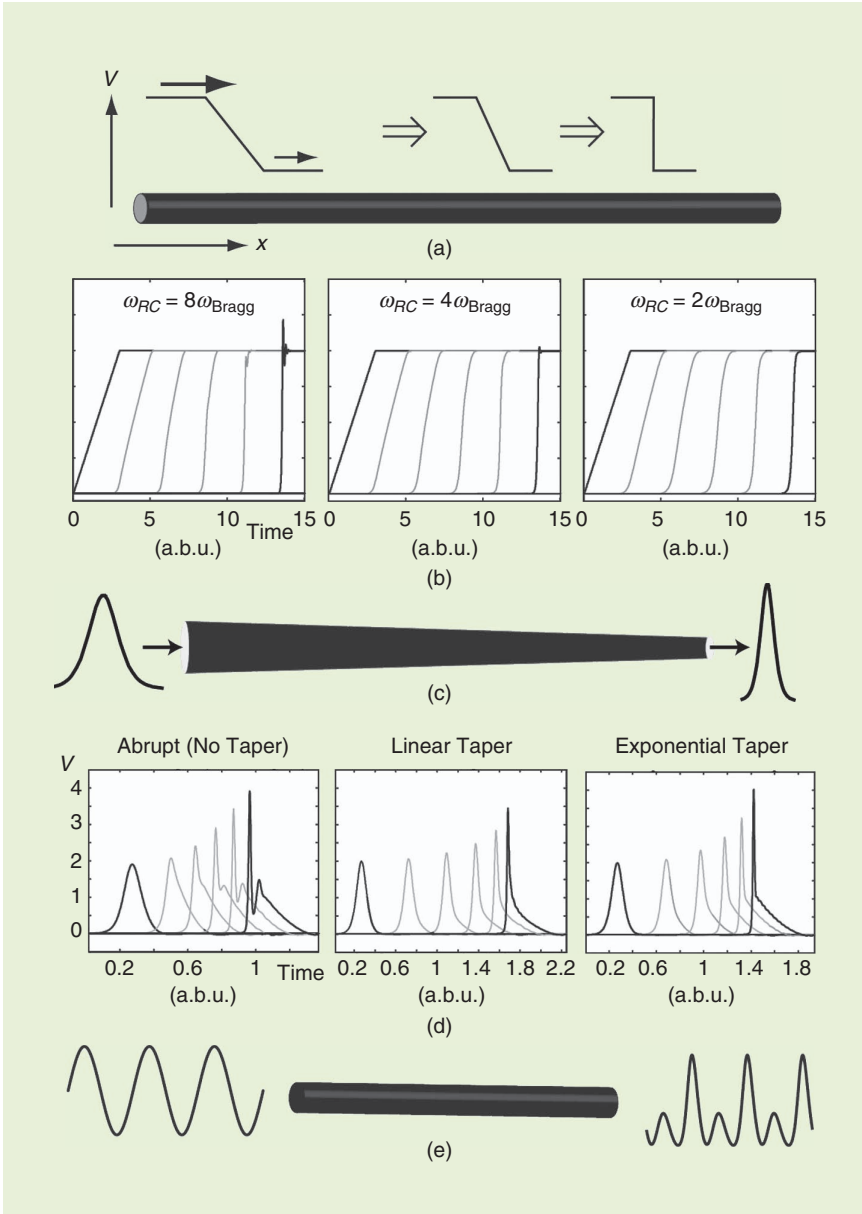

Figure 7. *(a) Edge sharpening using the NLTL, with (b) the simulation performed with a circuit simulator. (c) Ultrafast pulse generation with a tapered NLTL, with (d) the simulation performed with a circuit simulator. (e) Simulated harmonic generation.*

Ultrafast Pulse Generation

The formation of solitons on the NLTL from a nonsoliton input, which occurs in the weak loss regime ($w_{\text{Bragg}} \ll w_{RC}$), can be exploited to generate a fast pulse. Figures 3 and 4 show that the NLTL can convert a nonsoliton input pulse into one or more solitons, with some, if

not all, of these solitons being sharper than the initial input pulse. Of these, the tallest soliton is sharpest. In general, the key to generating a sharp pulse is to choose an input waveform that nests a tall, narrow soliton component and then to let it propagate on the NLTL. The tall (thus fast) soliton component will then emerge first from the initial waveform.

The win from the frequency-domain point of view is that the emergent tall, sharp soliton has higher spectral contents than the initial waveform. In fact, this tall, sharp soliton output will form close to the NLTL's intrinsic cutoff frequency, w_{Bragg}, where the dispersion is most pronounced, to effectively counteract the nonlinearity. The higher the w_{Bragg}, the sharper/taller the soliton will be. Therefore, a trick to further sharpen the soliton is to gradually taper down the NLTL by reducing L and C together and so gradually increase w_{Bragg}, while keeping the ratio of L to C constant so that the characteristic impedance of the NLTL remains constant. (Because C is voltage dependent, the previous statement is somewhat limited in terms of accuracy but overall is valid and captures the essential dynamics.) Such tapering will allow an increasingly sharper and taller soliton along the NLTL [Figure 7(c)].

Another way to understand this tapering is by considering the soliton that forms at the beginning of the NLTL as the low-frequency input to the next stage, which has a higher w_{Bragg}. This will pull out the tall soliton component associated with that higher w_{Bragg}, which will then be an input to the next stage with an even higher w_{Bragg}. (This sharpening process repeats itself along the tapered NLTL). This tapering strategy was used to create a fast pulse with only a 5-ps duration [9], which was then harnessed to construct a 500-GHz sampling system [4] for research and a 100-GHz commercial oscilloscope [21]. The NLTL tapering strategy has achieved pulse compression by a factor of 7 [11]. Figure 7(d) shows two different tapering scenarios––linear and exponential––for creating sharp pulses.

Broadband Harmonic Generation

The frequency conversion by the NLTL discussed in the preceding two sections is a nonlinear process. This nonlinear frequency conversion can also be leveraged to generate higher harmonics. Several commercial comb frequency generators have been developed based on this concept [23], [24]. The devices use an NLTL to convert a low-frequency sinusoid into a waveform with significant harmonics. The design of the NLTL for this application must satisfy the weak loss regime condition, $w_{\text{Bragg}} \ll w_{RC}$. Although harmonic generators using nonlinear elements are common, they often require narrowband filters. The NLTL provides a wideband-width frequency converter with very good conversion efficiency. Figure 7(e) shows a conversion efficiency of 64% from the first to second harmonics.

In general, the key to generating a sharp pulse is to choose an input waveform that nests a tall, narrow soliton component and then to let it propagate on the NLTL.

The Soliton Oscillator

The soliton pulse generation discussed in "Ultrafast Pulse Generation" section uses the NLTL as a two-port system, where an input waveform is required to generate the soliton pulse output. One meaningful departure from this approach would be to construct a one-port autonomous soliton oscillator by combining the NLTL with an amplifier in a positive feedback loop. Such a circuit would self-start from ambient noise and self-sustain its steady-state oscillation to produce a train of periodic solitons, requiring no high-frequency input to drive the system.

In 2006, Ricketts, Li, and Ham introduced such a self-sustained soliton oscillator by arranging an NLTL and a noninverting amplifier in a circular loop [Figure 8(a)] [25], [26]. The amplifier enables the initial start-up by amplifying ambient noise, and it compensates for system loss in the steady state, as is commonly done in sinusoidal oscillators [27]. The challenge, however, is that the continued amplification of random noise can generate many solitons with different amplitudes which will circulate in the loop at different speeds, colliding with one another. Each collision event introduces both momentary amplitude modulation and permanent time shift or phase modulation. To make matters worse, the amplifier can significantly distort a soliton (e.g., clipping of the soliton top), hence sending out the significantly nonsoliton pulse back onto the NLTL, which then can generate even more solitons of differing amplitudes [e.g., Figure 4(a)], thus causing more collisions and, hence, more amplitude and phase modulations. Consequently, although the circuit may be able to self-sustain an oscillation, the oscillating signal can become highly unstable, with varying amplitudes and unruly pulse repetition rates.

The solution offered by Ricketts et al. [25], [26] to address this instability is an adaptive amplifier that automatically lowers its bias point on the input-output transfer curve as the soliton oscillation grows [Figures 8(b)–(d)]. At the very beginning of the oscillation start-up, the amplifier bias is set in the middle of the transfer curve, where the tangential slope is sufficiently large so that small noise can be amplified. As the signal circulating in the loop grows into

taller pulses through this amplification, the amplifier pushes down its bias point into the attenuation portion of the transfer curve. With this lowered bias, small signals are now attenuated, and the higher portions of tall pulses are still amplified. This threshold-dependent gain-attenuation mechanism boosts the main tall solitons while suppressing small perturbing solitons created from ambient noise and distortion. Also, with the lowered bias, the amplifier output is kept out of clipping, so the distortion itself is reduced. In this way, the circuit removes solitons of smaller amplitudes that could otherwise collide with the main tall solitons and cause signal instabilities. Finally, as the main tall solitons continue to grow, the amplifier bias is driven deep into the attenuation region, and, thus, the overall gain experienced by the main

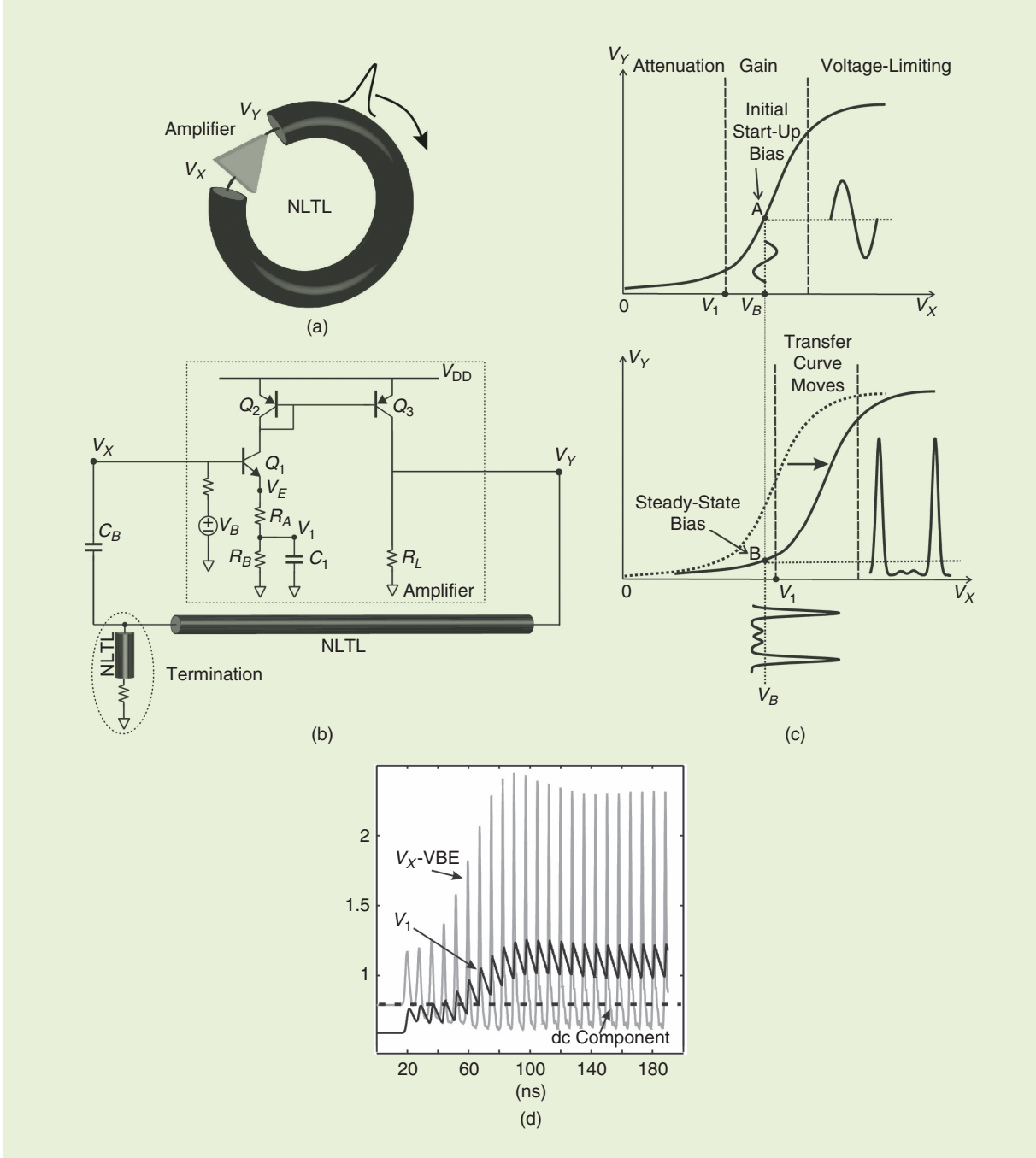

Figure 8. *(a) A circular soliton oscillator. (b) An example circuit for the circular soliton oscillator topology. (c) The amplifier features an automatic adaptive bias control. In the steady state, it presents a level-dependent gain-attenuation mechanism. (d) The measured soliton oscillation start-up transitions to steady-state oscillation. (Source: [25] and [26]; used with permission.)*

tall solitons is gradually reduced to a point that just balances the loss in the system, thus reaching steady-state oscillation. With this threshold-dependent gain attenuation, stability is ensured, and the oscillator robustly generates a periodic train of solitons with uniform amplitude.

After this general concept of the soliton oscillator was demonstrated with circular topology [25], [26], Yildirim, Ricketts, and Ham developed a reflection soliton oscillator topology in 2009 [28] (Figure 9). Here, the signal does not circulate in a loop but races back and forth on an NLTL with reflective terminations at both ends. Specifically, the oscillator consists of an NLTL, with one end open and the other end terminated with a one-port amplifier [Figure 9(a)]. In the steady state, a self-generated soliton travels back and forth on the NLTL (reflected at both ends of the NLTL). In the steady state, the one-port amplifier [Figure 9(b)] produces a negative output resistance for voltages beyond a particular threshold and a positive output resistance for voltages below the threshold. Thus, the reflection from the one-port amplifier provides gain for the main upper portion of the pulse to compensate for loss while attenuating small perturbations to ensure oscillation stability, just like in the circular topology case.

Because such level-dependent gain attenuation to suppress small signals cannot be used during the initial start-up (which must amplify small ambient noise), the one-port amplifier is also designed to realize an adaptive bias control [Figure 9(b)], as in the case of the circular topology circuit. This reflection soliton oscillator is a simpler build than the circular soliton oscillator, requiring only half the NLTL length to achieve the same pulse repetition rate. It is also free from the rather complex impedance-matching issue of the circular topology.

In terms of optimizing the phase noise performance, the soliton oscillator features two conflicting traits [29]. On one hand, the short duration of each soliton pulse reduces the time to interact with noise, thus tending to lower the phase noise. On the other hand, the amplitude-dependent speed of the soliton readily converts amplitude noise to phase noise, thus tending to increase the phase noise. Therefore, for overall phase noise optimization, this design tradeoff must be considered carefully.

The Chaotic Soliton Oscillator and Its Applications

The main design focus of the soliton oscillators [25], [26], [28] discussed in the preceding section was that

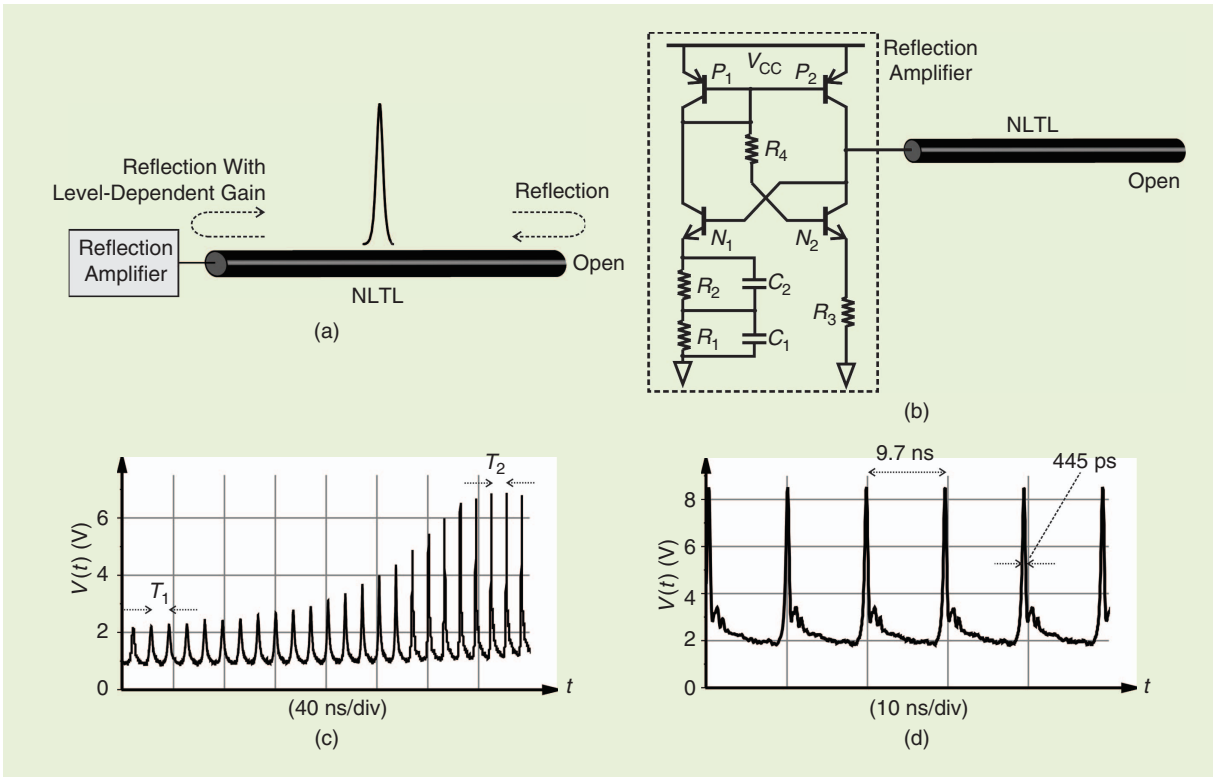

Figure 9. *(a) A reflection soliton oscillator. (b) An example circuit schematic for the reflection soliton oscillator. The one-port reflection amplifier presents a level-dependent gain–attenuation mechanism during steady-state oscillation. (c) and (d) The measured start-up and steady-state oscillation. (Source: [28]; used with permission.)*

The soliton has provided a fascinating glimpse into the world of nonlinearity for nearly 200 years.

the amplifier exhibits the level-dependent gain-attenuation mechanism. This allowed small perturbations to be suppressed while the main tall solitons were sustained against system loss, thereby preventing soliton collisions and stabilizing the signal dynamics into a robust periodic train of solitons [Figure 10(a)]. We can do exactly the opposite as well: if we design the amplifier to offer full gain at all signal levels, small perturbations, such as noise and dispersive tails, will grow out to form parasitic solitons of varying amplitudes, and these will keep colliding with one another as well as with the tall main solitons on the NLTL, continuing to cause amplitude and phase modulations, thus leading to chaos [Figure 10(b)].

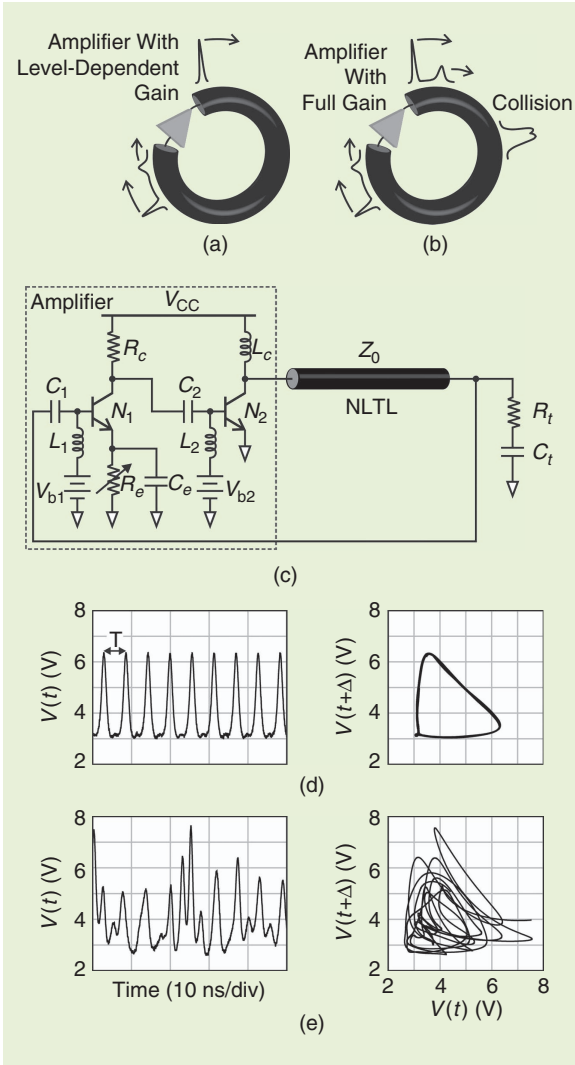

Figure 10. *(a) and (b) Depending on whether the amplifier presents a level-dependent gain or a full gain at all levels, the soliton oscillator can produce a stable periodic train of solitons or a chaotic signal. (c) An example soliton oscillator that can be tuned from the stable to the chaotic mode. (d) and (e) The measured data (time-domain signal and phase-space trajectory) of the circuit in its stable and chaotic modes. (Source: [30]; used with permission.)*

In 2014, Yildirim and Ham experimentally demonstrated such a chaotic soliton oscillator that works by promoting soliton collisions [30] [Figure 10(c)]. In this circuit, by lowering the value of the resistance R_e, the amplifier characteristic can be transitioned from level-dependent gain to full gain: in the former setting, soliton collisions are suppressed, yielding a stable soliton oscillation with the phase-space trajectory tracing a clear limit cycle [Figure 10(d)]; in the latter setting, soliton collisions are prevalent, resulting in characteristically chaotic oscillation [Figure 10(e)]. As the soliton oscillation transitions from periodic to chaotic with the lowering of R_e, we can observe bifurcations as well.

Chaotic circuits have been of pure and applied interest [31]–[33]. On one hand, they represent an easily accessible experimental platform for interrogating chaotic behaviors. On the other hand, chaotic circuits have found applications in random-number generation [32] and chaotic communication [33], [34]. The distinctive merit of the NLTL-based chaotic soliton oscillator over traditional chaotic circuits is its extremely large bandwidth, if implemented as an integrated circuit (e.g., with GaAs technology), which can support picosecond-long soliton pulses. Therefore, the chaotic soliton oscillator can be useful for broadband private chaotic communication. The simulations in Figure 11, performed by Yildirim, Sun, and Li [1, Ch. 11]) show the feasibility of using chaotic soliton oscillators for chaotic communication via transmitter–receiver synchronization.

Other Microwave Solitons Beyond the NLTL Solitons

This review article has focused on the KdV soliton dynamics supported on the NLTL and their applications in microwave engineering. Besides the NLTL, there are several other nonlinear dispersive systems that host KdV soliton dynamics. As mentioned in the introduction, one of the most well-known examples is water, where the soliton phenomenon was first discovered. Another KdV system example is plasma, where ion acoustic waves are particularly well known for their soliton modes; however, electron density waves may be able to have soliton modes as well. One interesting possibility for microwave application, then, is to use the solid-state 2D electron system, such as semiconductor quantum wells (e.g., GaAs/AlGaAs quantum wells) and graphene, which can propagate

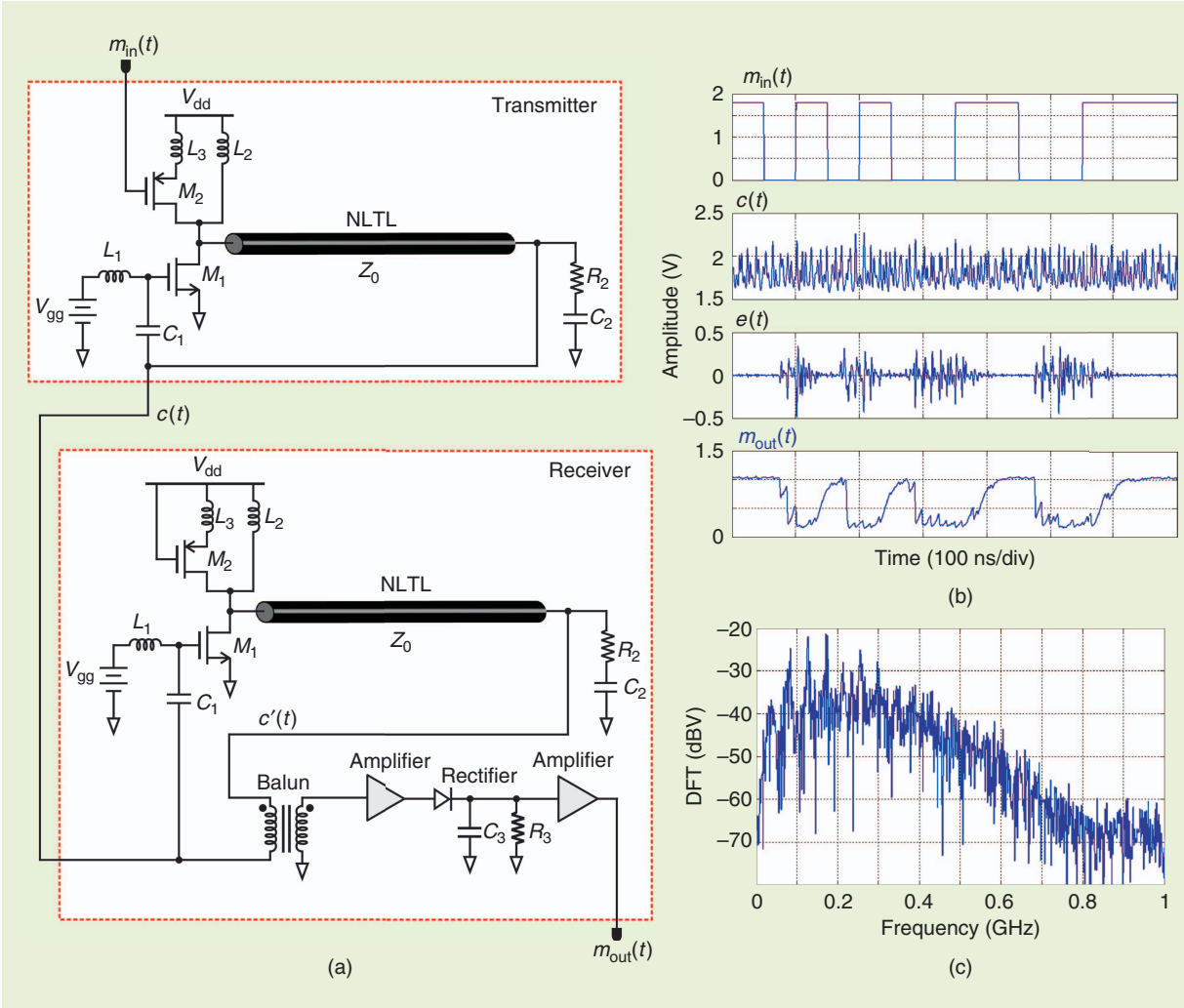

Figure 11. *(a) The schematic of chaotic communication with chaotic soliton oscillators and (b) the simulated transmission and reception of a square-wave signal. (c) The spectrum of the transmitted signal resembling random noise is not decipherable by receivers, which do not have a matching nonlinear system. DFT: discrete Fourier transform. (Source: [1, Ch. 11]; used with permission.)*

electron density waves at gigahertz frequencies [35]–[38]. Nonlinearity may be obtained with a strong excitation to tease the second-order nonlinearity or by combining the 2D electron systems with distributed varactors. The wavelength of 2D plasmonic waves can be hundreds of times smaller than the wavelength of electromagnetic waves in air [35]–[38]; thus, it would be interesting to interrogate solitons that are highly confined spatially.

There are other types of solitons besides KdV solitons. Two notable examples are spin-wave solitons [39] and optical solitons [40], both of which are based on the nonlinear Schrödinger equation, as opposed to the KdV equation. The nonlinear Schrödinger dynamics are highly interesting as well and different from the KdV dynamics in their details. However, the nonlinear Schrödinger equation still exhibits the key invariant eigenvalue structure, just as the KdV equation does. Spin-wave solitons occur in the microwave regime, so they provide another opportunity for microwave engineering.

Conclusions

The soliton has provided a fascinating glimpse into the world of nonlinearity for nearly 200 years. From its initial discovery as a solitary wave, to the towering development of the inverse scattering method, to its application for 500-GHz sampling systems, the soliton has offered both a window to the captivating mathematical structure underlying nonlinear physics and a practical tool for microwave systems. Recent developments of stable and chaotic self-sustained soliton oscillators bring new opportunities for understanding and leveraging the soliton's unique properties in microwave engineering. New applications may continue to develop, such as energy conversion exploiting the

high-energy pulses from the NLTL and soliton-based analog computation using protected eigenvalues. All of these are a tribute to the profound dynamics of the soliton and nonlinear waves.

Acknowledgment

Donhee Ham thanks Isik Kizilyalli, program director of the Advanced Research Projects Agency-Energy, for support under contract DE-AR0000858.

References

[1] D. S. Ricketts and D. Ham, *Electrical Solitons: Theory, Design, and Applications*. Boca Raton, FL: CRC Press, 2011.

[2] R. Landauer, "Shock waves in nonlinear transmission lines and their effect on parametric amplification," *IBM J. Res. Develop.*, vol. 4, no. 4, pp. 391–401, Oct. 1960. doi: 10.1147/rd.44.0391.

[3] J. R. Alday, "Narrow pulse generation by nonlinear transmission lines," *Proc. IEEE*, vol. 22, no. 6, p. 739, June 1964. doi: 10.1109/PROC.1964.3092.

[4] M. J. Rodwell et al., "Active and nonlinear wave propagation devices in ultrafast electronics and optoelectronics," *Proc. IEEE*, vol. 82, no. 7, pp. 1037–1059, July 1994. doi: 10.1109/5.293161.

[5] R. Y. Yu, M. Reddy, J. Pusl, S. T. Allen, M. Case, and M. J. W. Rodwell, "Millimeter-wave on-wafer waveform and network measurements using active probes," *IEEE Trans. Microw. Theory Techn.*, vol. 43, no. 4, pp. 721–729, Apr. 1995. doi: 10.1109/22.375217.

[6] D. W. van der Weide, "Delta-doped Schottky diode nonlinear transmission lines for 480-fs, 3.5-V transients," *Appl. Physics Lett.*, vol. 65, no. 7, pp. 881–883, Aug. 1994. doi: 10.1063/1.113013.

[7] M. J. W. Rodwell, M. Kamegawa, R. Yu, M. Case, E. Carman, and K. S. Giboney, "GaAs nonlinear transmission lines for picosecond pulse generation and millimeter-wave sampling," *IEEE Trans. Microw. Theory Techn.*, vol. 39, no. 7, pp. 1194–1204, July 1991. doi: 10.1109/22.85387.

[8] M. Case, M. Kamegawa, R. Y. Yu, M. J. W. Rodwell, and J. Franklin, "Impulse compression using soliton effects in a monolithic GaAs circuit," *Appl. Physics Lett.*, vol. 68, no. 2, pp. 173–175, Jan. 14, 1991. doi: 10.1063/1.104963.

[9] M. Case, "Nonlinear transmission lines for picosecond pulse, impulse and millimeter-wave harmonic generation," Ph.D. dissertation, Univ. California, Santa Barbara, CA, 1993.

[10] D. Salameh and D. Linton, "Microstrip GaAs nonlinear transmission-line (NLTL) harmonic and pulse generators," *IEEE Trans. Microw. Theory Techn.*, vol. 47, no. 7, pp. 1118–1122, July 1999. doi: 10.1109/22.775445.

[11] M. Tan, C. Y. Su, and W. J. Anklam, "7× electrical pulse compression on an inhomogeneous nonlinear transmission line," *Electron. Lett.*, vol. 24, no. 4, pp. 213–215, Feb. 1988. doi: 10.1049/el:19880143.

[12] A. C. Scott, F. Y. F. Chu, and D. W. McLaughlin, "The soliton: a new concept in applied science," *Proc. IEEE*, vol. 61, no. 10, pp. 1443–1483, Oct. 1973. doi: 10.1109/PROC.1973.9296.

[13] P. G. Drazin and R. S. Johnson, *Solitons: An Introduction*. Cambridge, U.K.: Cambridge Univ. Press, 1989.

[14] M. Toda, *Nonlinear Waves and Solitons*. Norwell, MA: Kluwer Academic Publishers, 1989.

[15] J. S. Russel, "Report on waves," in *Report 14th British Assoc. Advancement of Science Meeting*, York, U.K., Sept. 1844, pp. 311–390.

[16] D. J. Korteweg and G. de Vries, "On the change of form of long waves advancing in a rectangular canal, and on a new type of long stationary waves," *Philosoph. Mag.*, vol. 39, no. 240, pp. 422–443, 1895. doi: 10.1080/14786449508620739.

[17] N. J. Zabusky and M. D. Kruskal, "Interactions of solitons in a collision-less plasma and the recurrence of initial states," *Physics Rev. Lett.*, vol. 15, no. 6, pp. 240–243, 1965. doi: 10.1103/PhysRevLett.15.240.

[18] R. Miura, "Korteweg-de Vries equation and generalizations. I. A remarkable explicit nonlinear transformation," *J. Math. Physics*, vol. 9, no. 8, pp. 1202–1204, 1968. doi: 10.1063/1.1664700.

[19] C. Gardner, J. Greene, M. Kruskal, and R. Miura, "Method for solving the Korteweg-de Vries equation," *Physics Rev. Lett.*, vol. 19, pp. 1095–1097, Nov. 1967. doi: 10.1103/PhysRevLett.19.1095.

[20] P. Lax, "Integrals of nonlinear equations of evolution and solitary waves," *Commun. Pure Appl. Mathematics*, vol. 21, pp. 467–490, Sept. 1968. doi: 10.1002/cpa.3160210503.

[21] S. H. Pepper and K. Schoen, "NLTLs push sampler products past 100 GHz," *Microwaves and RF*, Oct. 2005. [Online]. Available: https://www.mwrf.com/components/nltls-push-sampler-products-past-100-ghz

[22] K. Noujeim, J. Martens, and T. Roberts, "Frequency-scalable nonlinear-transmission-line-based vector network analyzers," 2012. [Online]. Available: https://www.armms.org/media/uploads/1335467233.pdf

[23] MarkiMicrowave, Inc., Morgan Hill, CA, USA, 2017. [Online]. Available: https://www.markimicrowave.com/Assets/datasheets/NLTL-6273.pdf

[24] MACOM, Lowell, MA, USA. [Online]. Available: https://www.macom.com/products/frequency-generation/nltl-gaas-comb-generators

[25] D. Ricketts, X. Li, and D. Ham, "Electrical soliton oscillator," *IEEE Trans. Microw. Theory Techn.*, vol. 54, no. 1, pp. 373–382, Jan. 2006.

[26] D. Ricketts, X. Li, N. Sun, K. Woo, and D. Ham, "On the self-generation of electrical soliton pulses," *IEEE J. Solid-State Circuits*, vol. 42, no. 8, pp. 1657–1668, Aug. 2007.

[27] W. Andress and D. Ham, "Standing wave oscillators utilizing wave-adaptive tapered transmission lines," *IEEE J. Solid-State Circuits*, vol. 40, no. 3, pp. 638–651, Mar. 2005.

[28] O. O. Yildirim, D. Ricketts, and D. Ham, "Reflection soliton oscillator," *IEEE Trans. Microw. Theory Techn.*, vol. 57, no. 10, pp. 2344–2353, Oct. 2009. doi: 10.1109/TMTT.2009.2029025.

[29] X. Li, O. O. Yildirim, W. Zhu, and D. Ham, "Phase noise of distributed oscillators," *IEEE Trans. Microw. Theory Techn.*, vol. 58, no. 8, pp. 2105–2117, Aug. 2010. doi: 10.1109/TMTT.2010.2053062.

[30] O. O. Yildirim and D. Ham, "High-dimensional chaos from self-sustained collisions of solitons," *Appl. Physics Lett.*, vol. 104, no. 24, pp. 244109-1–244109-4, 2014. doi: 10.1063/1.4884943.

[31] L. O. Chua, C. Wu, A. Huang, and G. Zhong, "A universal circuit for studying and generating chaos. I. Routes to chaos," *IEEE Trans. Circuits Syst.*, vol. 40, no. 10, pp. 732–744, Oct. 1993.

[32] T. Stojanovski, J. Pihl, and L. Kocarev, "Chaos-based random number generators. Part II: practical realization," *IEEE Trans. Circuits Syst.*, vol. 48, no. 3, pp. 382–385, Mar. 2001. doi: 10.1109/81.915396.

[33] K. Cuomo and A. Oppenheim, "Circuit implementation of synchronized chaos with applications to communications," *Physics Rev. Lett*, vol. 71, no. 1, pp. 65–68, July 1993.

[34] D. Ham, X. Li, S. Denenberg, T. H. Lee, and D. S. Ricketts, "Ordered and chaotic electrical solitons: Communication perspectives," *IEEE Comm. Mag.*, vol. 44, pp. 126–135, Dec. 2006.

[35] H. Yoon et al., "Measurement of collective dynamical mass of Dirac fermions in graphene," *Nature Nanotechnology*, vol. 9, pp. 594–599, Aug. 2014. doi: 10.1038/nnano.2014.112.

[36] H. Yoon, K. Yeung, V. Umansky, and D. Ham, "A Newtonian approach to extraordinarily strong negative refraction," *Nature*, vol. 488, pp. 65–69, Aug. 2012. doi: 10.1038/nature11297.

[37] W. Andress et al., "Ultra-subwavelength two-dimensional plasmonic circuits," *Nano Letters*, vol. 12, no. 5, pp. 2272–2277, May 2012. doi: 10.1021/nl300046g.

[38] H. Yoon, K. Yeung, P. Kim, and D. Ham, "Plasmonics with two-dimensional conductors," *Philosoph. Trans. Roy. Soc. A*, vol. 372, p. 20130104, Mar. 2014. doi: 10.1098/rsta.2013.0104.

[39] M. Wu, B. A. Kalinikos, and C. E. Patton, "Self-generation of chaotic solitary spin wave pulses in magnetic film active feedback rings," *Physics Rev. Lett.*, vol. 95, no. 23, pp. 237202-1–237202-4, Nov. 2005. doi: 10.1103/PhysRevLett.95.237202.

[40] H. A. Haus and W. S. Wong, "Solitons in optical communications," *Rev. Modern Physics*, vol. 68, no. 2, pp. 423–444, Apr. 1996. doi: 10.1103/RevModPhys.68.423.